Blending and Suspension Characteristics of VISCO JET Impellers

A. Krupica* **and T. Jirout**
Czech Technical University in Prague,
Faculty of Mechanical Engineering,
Department of Process Engineering,
Technická 4, Prague, Czech Republic

doi: https://doi.org/10.15255/CABEQ.2025.2427

Original scientific paper
Received: April 30, 2025
Accepted: July 1, 2025

Visco Jet® impellers have been available for several years and are marketed as an alternative to other standard impeller types, such as pitched blade impellers, Rushton turbines, or hydrofoils. However, their performance has not yet been evaluated in the scientific literature. This article aims to address this gap by reviewing two basic Visco Jet® impeller types: the Classic and the Spiral.

The impellers are characterised by dimensionless parameters, specifically, the Power number, dimensionless mixing time, and suspension power input. Their performance is evaluated based on dimensionless homogenisation energy and the dimensionless suspension power input in the just-suspended state. Measurements were carried out using methods described in the Handbook of Industrial Mixing. The results suggest that Visco Jet® impellers perform comparably to other standard impellers, particularly in the creeping flow regime. Their main advantages appear to be ease of use and reduced torque requirements.

Keywords
energy comparison, Visco Jet, suspension, blending, homogenisation

Introduction

In recent years, the impellers examined in this study have seen increased industrial use, particularly in applications such as paint dispersion and food or beverage processing. They are often favoured for initial homogenisation of the input material, with manufacturers claiming improved product quality and cost reduction. However, apart from Rahimi *et al.*[1], who conducted limited tests on sets of impellers similar in geometry to the Visco Jet® Classic, no substantial performance data exist in the literature for impellers with geometry similar to the Visco Jet® impellers. The manufacturer, VISCO JET®, claims their impellers offer several advantages, including *'Increased process efficiency due to short agitating times and quick and easy cleaning'* and *'Reduced process costs due to low energy costs and faster throughput times in the production process'* across various viscosities[2]. From an engineering perspective, this absence of fundamental performance data is concerning. A clear understanding of key characteristics is essential for the effective design of any stirred system[3]. Among these characteristics, the relationship between flow behaviour, homogenisation time, and power consumption is essential, as it provides engineers with an energy value based on which the various impellers can be evaluated. However, the manufacturer provides no quantitative performance data for their impellers, apart from some basic information, such as dimensions, declared suitability for large vessels, mixing through combination of laminar and turbulence inside the cone, apparently radial-axial flow pattern, and suitability for media with viscosity up to Pa s and 100 Pa s (depending on the impeller type)[2], which is interesting given the dimensions and shape of the impellers. For such high-viscosity fluids, more conventional impellers such as ribbons, screws, or anchors, are typically recommended[3]. Compared to the proposed Visco Jets, they are substantial in size and prefer to operate at slow rotation speeds. Moreover, these specialised impellers are not recommended for the use with low-viscosity fluids. For such applications, more optimized axial-flow hydrofoils are preferred[3]. Either case, no impeller with geometry similar to that of the Visco Jets was found.

Taking into account the absence of literature data and the unique design of the Visco Jet® impellers, a series of experiments was conducted to evaluate their behaviour using established methodologies. The goal of these experiments is to explore the basic behaviour of the impellers using a standard

*Corresponding author: adam.krupica@fs.cvut.cz

methodology comparable to other articles. Based on these results, further engineering evaluations can be made, or more in-depth research can be performed. With this goal in mind and based on previous experience, a set of suitable measurement methods was selected from the Handbook of Industrial Mixing[3]. The results of these experiments are presented in this article, along with a comparison with those of other standard impellers.

Materials and methods

As stated in the Introduction, several performance characteristics of the Visco Jets® impellers must be measured to enable meaningful evaluation. All measurements followed the methodology recommended in the Handbook of Industrial Mixing[3]. The gathered data were subsequently statistically analysed and plotted against other impellers and agitators for which comparable results were available in the published literature. To enhance the clarity of the article, the various measurements are defined in their respective subchapters. A range of Newtonian model fluids with varying viscosities were used: glucose syrup, glycerol, and water. These were selected to represent the anticipated range of materials on which the impellers were expected to operate. The exploration of other materials that were more viscous was considered; however, the anticipated mixing times were deemed too long for reliable evaluation. The viscosity of these fluids was set, sometimes repeatedly as required by certain measurements, using an Anton Paar MCR 102 rheometer with concentric cylinder geometry. The fluid was tempered on the rheometer to 21±0.2 °C according to the experiment temperature. To keep the temperature constant, the experiments were carried out in a temperature-controlled laboratory. The experiments temperature was monitored throughout the study. The initial viscosity of the model fluids was 6.1 Pa s for glucose syrup, 1.1 Pa s for glycerol and 1.2 mPa s for water. These values remained constant during power input measurements, but slowly decreased over time during blending measurements due to dilution from the indicator solution. All experiments were conducted in the same cylindrical, flat-bottom vessel with an inner diameter T of 0.2 m and $H/T = 1$. The effect of baffles with a standard width $W_b = 0.1T$ and thickness of 1 mm was also explored. A standard configuration of four baffles positioned at 90° intervals was employed. The off-bottom clearance of the baffles is characterised by the dimension L. This distance was usually set to 0; however, during suspension experiments, the position of 0.4 was tried based on the preliminary results.

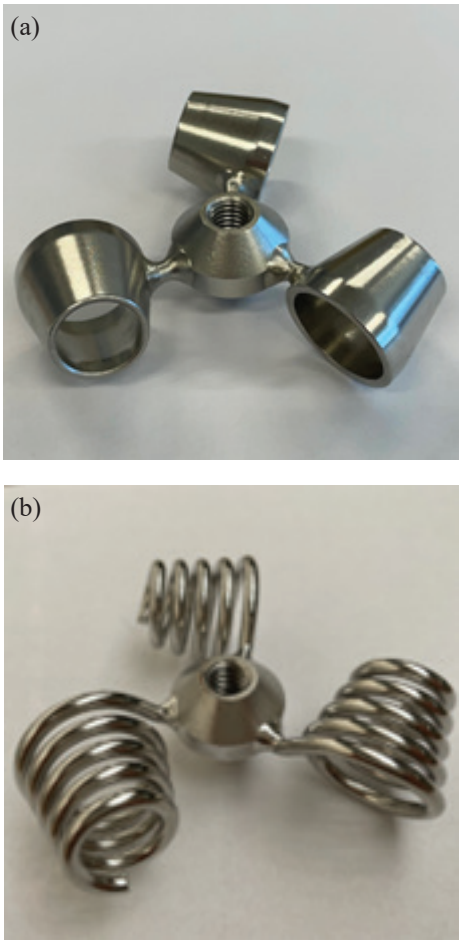

Fig. 1 – *Illustration of the cone structure of the two different Visco Jet® impellers: (a) Visco Jet® Classic, (b) Visco Jet® Spiral*

The diameter of the impeller was set at 0.06 m. This value was obtained as twice the distance between the axis and the centre of the larger cone opening. Two types of impeller were tested: Visco Jet® Classic and Visco Jet® Spiral. The primary distinction between these impellers lies in the design of the mixing cones (see Fig. 1) with the remaining dimensions shared between them.

To illustrate the methodology employed in the collection of the data presented, a schematic representation of the general experimental setup is provided in Fig. 2.

Power input measurement

The power input was measured and subsequently converted into a dimensionless Power number (Po) using the torque measurement method. The measurement was carried out using a torque sensor (precision ± 0.5 Nm) and a tachometer attached to the shaft of the impeller. The data were collected using a programmable logic controller and interpreted using an Excel script.

The number of revolutions per minute (rpm) was set at the start of the experiment and was monitored on the control panel. In subsequent calculations, the rotation speed was considered constant, as it oscillated only about 2 rpm (0.033 s^{-1}) around the set value. The torque value was converted from the electric potential measured on the sensor. A range of rotation speeds was tested with 30 s delays after each change in their value to account for the inertia of the system. Three measurements were taken at a given rotation speed. The torque value measurement consisted of 400 values taken over a 10 s interval. To determine the drag from other mechanical parts, the torque value of the free-spinning impeller was also measured at each rotation speed and subtracted from the measured value. Such a measurement was carried out for both impeller types. Measurement was calibrated using a known Power number, geometry, and impeller setup with the 6 pitch-bladed impeller for which the available results were published by Medek and Fořt[4]. Three baffle configurations were tested: no baffles, standard baffles with $L/H = 0$, and raised baffles with $L/H = 0.4$. The last configuration was measured later, specifically for suspension evaluation.

Subsequently, the results were plotted and evaluated in their dimensionless form using MATLAB software, with the curve fitting toolbox utilising the function defined by Eq. 1. A 95 % confidence interval was established. The influence of the BP parameter was tested using Student's T-test. When unnecessary, an approximation was employed using an average value.

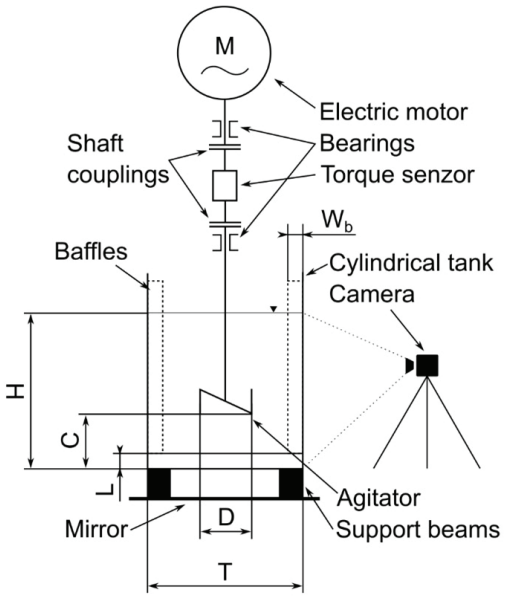

Fig. 2 – *Schematic of the measurement setup*

$$\mathrm{Po} = A_P \mathrm{Re}^{-B_P} \tag{1}$$

where, A_P and B_P represent the regression parameters, Re is the impeller Reynolds number, and Po is the Power number.

Finally, the relative torque of the two impellers was calculated. This parameter is often overlooked in most impeller evaluations; however, it is an important parameter since the torque required by the agitator significantly influences the design of support structures (size of load bearings, mounting beams, and tank supports) and of the drive system (motor, gearbox, various couplings, and shaft). This, in turn, has a significant influence on the initial cost of the equipment (CAPEX), as a more robust structure is required to support higher torque values.

As the torque value is dependent on the specific dimensions and general configuration of a system, a relative value is presented, with the results for Visco Jet® Classic being used as a reference. The relative torque values were calculated using the Power number, and blending time correlations using the acquired results and data found in the literature. Firstly, for a given system, with defined fluid properties, dimensions, and required blend time, the corresponding impeller Re number was found from a known dimensionless blend time. Based on its value, using the corresponding Po number and rotation speed, the required torque value can be calculated. For the results to be comparable, all system parameters, apart from impeller diameters, were assumed to be constant. The impellers were sized according to the specifications given for their defining regressions.

Blending time and homogenisation energy

Blending time was set using the iodine-thiosulphate starch indicator colorimetric method, selected for its ability to visualise the flow and the blending process throughout the batch. This is aided by the sharp contrast between the coloured and discoloured regions, as well as its suitability for working with all the model fluids[3].

An alternative method based on the change in fluid conductivity was also considered, but rejected due to the lack of prior knowledge of the system's behaviour, which made accurate probe placement impossible. The indicator was always injected at the same position beneath the fluid surface, close to the vessel wall, approximately midway between the baffles (if present). This location was selected as the worst-case injection position. Its placement is also unaffected by the large axial vortex present in the unbaffled configurations, making the two experiments more comparable. However, under creeping flow conditions, injection near the shaft could present similar challenges. For most experiments, the

impeller position was set at C/D = 1. However, based on the preliminary results and out of curiosity, a more distant placement toward the centre of the vessel (C/H = 0.5) was also tested, as it appeared likely to reduce the mixing time.

This hypothesis proved correct; nevertheless, due to the limited dataset, these results are provided for informational purposes only. Two baffle configurations were tested: one without baffles and another with baffles in contact with the bottom of the vessel (L/H = 0).

All blending experiments were recorded using a digital camera in time-lapse mode, capturing one frame per second for blending times exceeding 20 s, and four frames per second for shorter blending times. This frequency was deemed sufficiently precise for the given durations of the experiments. Longer intervals between frames were found to improve the repeatability of the measurements due to the greater contrast between frames. The blending time was defined as the time elapsed between the frame showing the end of the thiosulphate solution injection and the frame in which the liquid had returned to its original colour throughout its entire volume. Experiments were repeated at least four times for each rotation speed. To be accepted, measurements had to fall within 10 % of the average value for a given rotation speed, with at least three such acceptable measurements required. Data points not meeting these criteria were discarded. To further reduce subjective bias, the recordings were independently reviewed by the authors and their colleagues. The final value was set as the average of all evaluations. However, it should be noted that the results include the subjective interpretation of the authors and may differ if assessed by another researcher.

As the viscosity of most of the model fluids was modified by the addition of the indicator, it was re-measured following each set of measurements for a given rotation speed. The final viscosity for each set was determined as the average of the two bounding values, which was considered sufficiently accurate given the blending measurement technique.

The results were then plotted in dimensionless form and fitted using the regression curve defined by Eq. 2, along with a 95 % confidence interval, using MATLAB software. The influence of the B_B parameter was tested using Student's T-test. When deemed unnecessary, an approximation using an average value was used instead.

$$nt_B = A_B \mathrm{Re}^{-B_B} \tag{2}$$

where, A_B and B_B are the regression parameters, Re is the impeller Reynolds number, n is rotation speed, and t_B is measured blending time.

$$\frac{Pt_B^3}{\rho T^5} = \mathrm{Po} \cdot \left(nt_B\right)^3 \left(\frac{D}{T}\right)^5 \tag{3}$$

$$\frac{Pt_B^2}{\mu T^3} = \mathrm{Po} \cdot \left(nt_B\right)^{-1} \left(\frac{T}{D}\right)^2 \tag{4}$$

$$\frac{T^2 \rho}{\mu t_B} = \mathrm{Re} \cdot \left(nt_B\right)^{-1} \left(\frac{T}{D}\right)^2 \tag{5}$$

The evaluation of impeller performance was carried out by employing the dimensionless homogenisation energy, as defined in Eqs. 3 and 4 proposed by Rieger *et al.*[5]

Eq. 3 is particularly well-suited for the characterisation of turbulent flow, as it is designed to yield easily comparable constant values in fully developed turbulent flow. Meanwhile, Eq. 4 provides analogous results in the creeping flow region. The values obtained are then plotted as a function of the dimensionless criterion defined by Eq. 5, which consolidates all typical design parameters (fluid density and viscosity, system size, and mixing intensity) into a single value.

Suspension power input

The suspension power input was measured at the just-suspended state, as defined by the Zwietering condition[6]. For these experiments, a water and glass bead suspension was prepared. The diameter of the glass beds was 0.246 mm, with a density of 2500 kg m^{-3}. Two volumetric fractions of particles were tested, namely 2.5 % and 10 %. The suspension state was assessed visually, using a mirror placed beneath the vessel (as illustrated in Fig. 2), enabling observation of the behaviour across the entire tank bottom. Various impeller clearances from the vessel bottom were tested, namely C/D = 1, 0.75 and 0.5. The effect of baffle placement was also evaluated. The position of the baffles was varied solely in the vertical direction, characterised by the distance. The tested baffle positions were L/H = 0.05 and 0.4. The variant without baffles inside the vessel was also examined. The slightly raised position (L/H =0.05) of the baffles was selected based on the findings by Myers *et al.*[7], who demonstrated that a gap equivalent half the width of the baffle enhances the suspension capabilities of most impeller designs by eliminating "deadzones" caused by inadequate fluid flow in the baffle wake near the tank bottom. The subsequent exploration of the second off-bottom clearance was guided by the observations made on the baffled and unbaffled variants.

The measurement method, once again based on visual assessment of the stirred vessel, was repeated at least four times for every configuration. Each measurement commenced from a state of rest, with all particles settled at the base of the tank. The rota-

tion speed was gradually increased in steps of 25 rpm (0.417 s^{-1}), with 30-second pauses between each step to account for the system's inertia, until the Zwietering condition was met for all particles visible at the base of the vessel. The experiment was observed by both authors, and the rotation was increased until both agreed that the just-suspended state had been reached. However, due to the subjective nature of this measurement, different results may be obtained by other researchers. The repeated measurements were within 10 % of the average value of the given configuration, based on at least three measurements. To compare these results with those obtained using other impellers, the dimensionless power input was used as defined in Eq. 6, proposed by Riger and published by Jirout and Rieger[8].

The calculations were performed using the Power number correlations outlined in the Section Power input measurement, with the modified Froude number Fr' being calculated using Eq. 7, as presented by Rieger and Ditl[9]. The parameters used in these equations include suspension density ρ_{su}, liquid density ρ, gravitational acceleration g, and the difference between the solid and liquid densities $\Delta\rho$.

$$\pi_S = \frac{P}{\rho_{su}}\left(\frac{\rho}{g\Delta\rho}\right)^{\frac{3}{2}}\left(\frac{1}{T}\right)^{\frac{7}{2}} = \mathrm{Po}\cdot(\mathrm{Fr}')^{\frac{3}{2}}\left(\frac{D}{T}\right)^{\frac{7}{2}} \quad (6)$$

$$\mathrm{Fr}' = \frac{\rho n^2 D}{g\Delta\rho} \quad (7)$$

The results for the modified Froude number are typically correlated in a manner similar to that of the dimensionless blending time or Power number[8]. However, to achieve this correlation, it would be necessary to conduct a greater number of experiments, incorporating a wider range of configurations with varying particle size and density differences.

Results

Power input results

The results of the power input measurements, including fitted regressions and 95 % confidence intervals, are presented in Figs. 3a and 3b. Given the differing viscosities of the model fluids, the results can be categorised into two distinct groups. Fig. 3a shows results at low impeller Reynolds numbers (below Re of 200), obtained using more viscous glucose syrup and glycerol. Fig. 3b presents results at higher impeller Reynolds numbers (above Re of 10^3), measured with water.

The regression parameters for the correlations in Figs. 3a and 3b are listed in Table 1, along with their respective intervals of validity and estimated precision. According to the underlying theory, different flow regimes can be observed as the Reynolds number changes. Both Visco Jet® impellers achieved fully developed turbulence at Re values above 10^4, as shown in Fig. 3b. Unexpectedly, the power input for baffled systems was lower than for unbaffled ones for both impeller types. This outcome is noteworthy, as it contrasts with the behaviour typically observed with other impellers. Furthermore, the Power number appeared largely unaffected by the axial position of the baffles. All measurements in the raised configuration were within 10 % of the average value of 2.68, which is close to the value of 2.63 observed for the standard baffle position.

The observed increase follows the trend between the baffled and unbaffled configurations, as shown in Table 1. Consequently, the results related to the raised baffles have been excluded from the figure, as they overlapped with those of the standard baffled system.

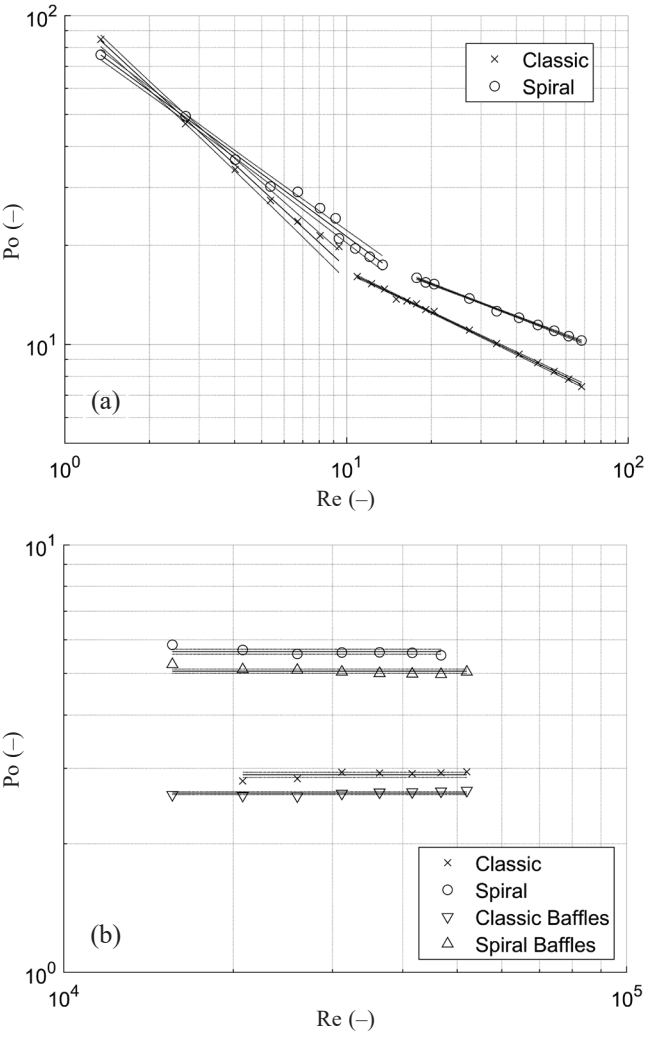

Fig. 3 – *Results of power input measurement presented through Power number as a function of (a) low impeller Reynolds number, (b) high impeller Reynolds number*

Table 1 – *Regression parameters for Power number calculation*

Impeller type	Baffles	A (–)	B (–)	Re range (–)	R^2
Visco Jet® Classic	none	110	0.79	1 – 10	0.99
	none	43	0.41	10 – 100	0.99
	none	2.90 ± 0.04	0	above $2 \cdot 10^4$	
	standard	2.63 ± 0.02	0	above 10^4	
	L/H = 0.4	2.68 ± 0.04	0	above 10^4	
Visco Jet® Spiral	none	91	0.63	1 – 10	0.99
	none	41	0.33	10 – 100	0.99
	none	5.63 ± 0.08	0	above 10^4	
	standard	5.07 ± 0.06	0	above 10^4	

Blending time

Similarly, blending time measurement results with proposed regressions and 95 % confidence intervals are shown in Figs. 4a and 4b. The corresponding regression parameters are presented in Table 2. Compared to the power measurement, more erratic results were obtained, which could be explained by the imprecise nature of the experiment due to short measurement times, especially at high Re values. At low impeller Reynolds numbers (as presented in Fig. 4a) there appears to be minimal difference between the performances of the two Visco Jet® impellers. Notably, the elevated impeller position exhibited a substantial enhancement in homogenisation times compared to the more traditional position of an impeller diameter above the vessel's bottom. This position is generally discouraged for radially pumping impellers due to the aeration from the fluid surface. Moreover, it has been shown that higher impeller positions tend to increase both homogenisation time[10] and Power number[11,12]. However, those results apply to fully developed turbulent flow, and our results suggest that the behaviour in the creep region may differ. At high Reynolds numbers, the results for the baffled configuration were again unexpected. In this case, the homogenisation time was longer in configurations with baffles, while the opposite behaviour was generally observed for other impellers. Our theory is that Visco Jet® impellers perform better when the circulation loop is allowed to fully develop without obstruction across the entire volume. The development of a tangential flow seems to also play a role in the process, as a similar behaviour was observed in suspension characteristics discussed later in the Section Suspension results. However, the precise reason

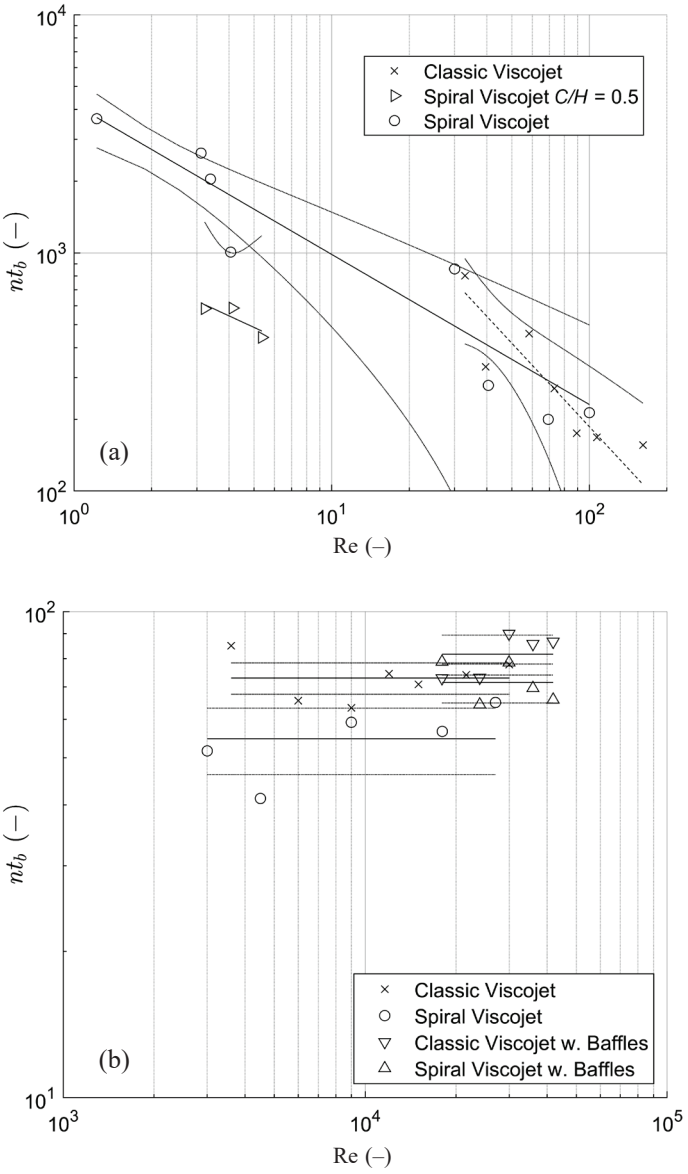

Fig. 4 – *Blending time measurement results presented through dimensionless homogenisation time as function of (a) low impeller Reynolds number, and (b) high impeller Reynolds number*

Table 2 – *Regression parameters for dimensionless blending time calculations*

Impeller type	Baffles	A (–)	B (–)	Re range (–)	R^2
Visco Jet® Classic	none	$3.98 \cdot 10^4$	1.2	30 – 200	0.76
	none	73.0 ± 5.3	0	above $3 \cdot 10^3$	
	standard	81.7 ± 7.7	0	above $2 \cdot 10^4$	
Visco Jet® Spiral	none	$4.2 \cdot 10^3$	0.63	1 – 100	0.91
(C/H = 0.5)	none	$1.1 \cdot 10^3$	0.5	4 – 7	0.71
	none	54.8 ± 8.5	0	above $4 \cdot 10^3$	
	standard	71.4 ± 6.6	0	above $2 \cdot 10^4$	

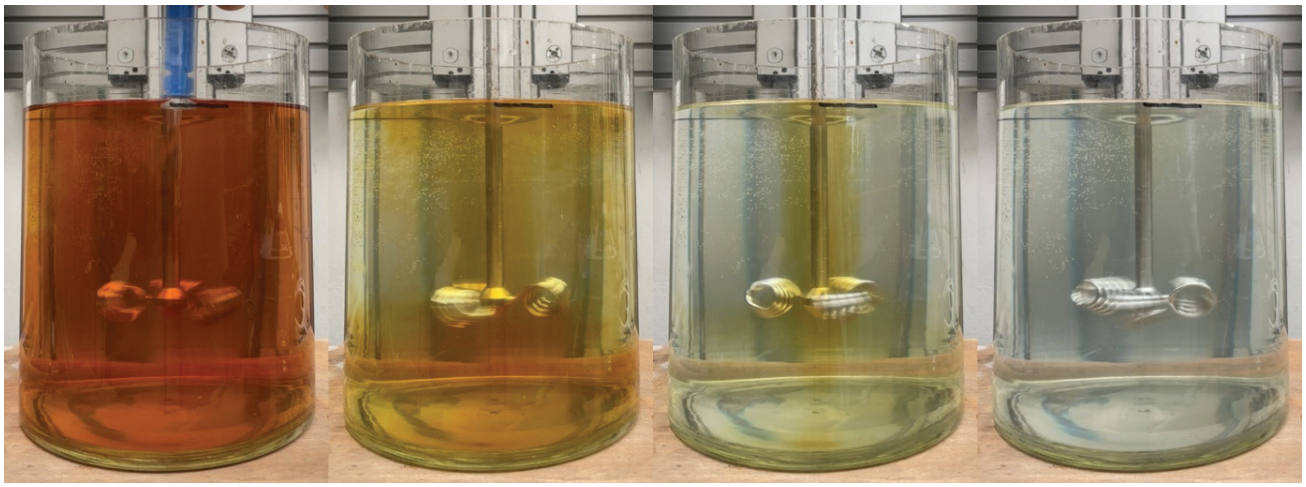

Fig. 5 – *Illustration of the blending process with Visco Jet® Spiral in low viscosity fluid (1 mPa s)*

for this phenomenon is yet unclear. During discolouration experiments illustrated in Fig. 5, the final homogenised regions were typically in proximity of the fluid surface and near the shaft. In systems without baffles, this position shifted with the creation of the axial vortex towards the vessel wall. Both impellers possess circulation loops of a similar nature, generating macroscopic flow analogous to those produced by other radially pumping impellers. Minor discrepancies were identified between the two impellers; however, these were considered inconsequential for the present study.

Suspension results

As outlined in Material and methods section, three distinct baffle configurations were examined in the suspension experiments. Initially, configurations with and without standard baffles were investigated. The unbaffled configuration with the highest off-bottom clearance of the impeller proved to be the most power-efficient configuration for achieving the just-suspended state. However, its performance was significantly limited by the formation of a large axial vortex, which restricted the the achievable impeller rotation speed. This lower rotation speed, combined with the strong tangential flow, impaired the impeller's performance, resulting in only 75–90 % of the vessel height being reached by the boundary of the particle cloud. The configuration with slightly raised baffles was found to be capable of fully homogenising the suspension; however, this was achieved at the expense of higher power input at the just-suspended state, as it necessitated higher rotation speed.

Based on these observations, the configuration with partially submerged baffles was proposed as it promised to disrupt the strong tangential flow at higher rotation speed while preserving the lower power input requirements to reach the just-suspended state. It proved to be effective in achieving both of these objectives. The effect of suspension concentration on the power required to achieve the just-suspended state was only observed to affect the standard baffled configuration. For the others, the results between the two tested concentrations were within the error margin of the measurement. To simplify the graphs, the results were merged into one data point when appropriate. The graphical representation of the dimensionless power input to achieve the just-suspended state is presented in Fig. 6.

Discussion

Assessing the validity of the results is challenging due to the absence of a comparable data set in the current literature. The only identified article, published by Rahimi *et al.*[1], defines the optimal geometrical configuration for the Visco Jet-type impeller.

However, this article presents only normalised values between their tested geometries, which are not applicable to our study. Consequently, a comparison of the presented results with those available for other impeller types suggests that our results are within a plausible range. The validity of the measurements is increased further by the fact that all the measurements were initially calibrated and tested with a well-defined impeller (6 Pitched-blade impeller).

Both impellers display in their blending process a typical double circulation loop observed with other radially pumping impellers, such as Rushton turbines or flat blade turbines[11]. This finding contradicts manufacturer claims of a radial-axial flow pattern, yet agrees with the numerical simulations conducted by Rahimi *et al.*[1]

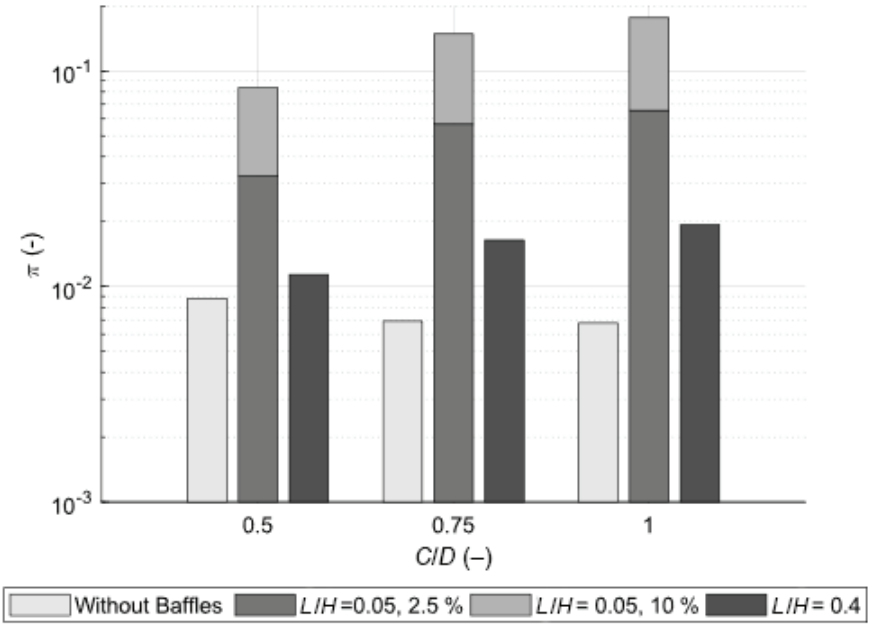

Fig. 6 – *Comparison of dimensionless suspension Power numbers for various baffle configurations and impeller of bottom clearances*

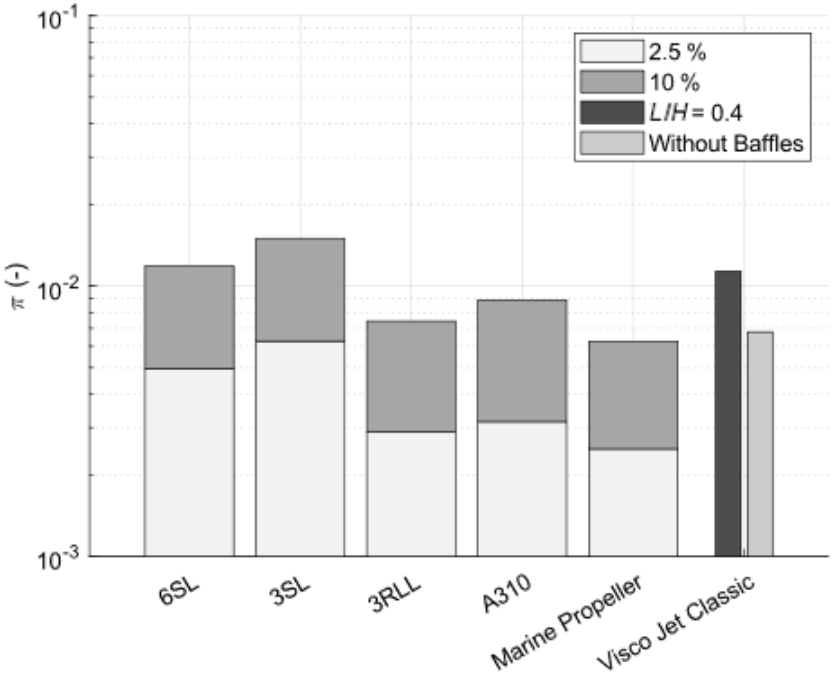

Fig. 7 – *Comparison of the dimensionless suspension Power number of the Visco Jet® Classic impeller with other standard impellers. Comparison data sourced from Jirout and Rieger[8]. The naming scheme of the impellers matches that in the cited article.*

As introduced in the Section Blending time and homogenisation energy, the dimensionless energy was used for the subsequent comparison to other standard impellers using the regressions from Tables 1 and 2. The results for the high Reynolds numbers (above 10^4) are presented in Table 3, along with a comparison with other impellers in standard operating conditions. The behaviour in the region of low Reynolds numbers (below $2 \cdot 10^2$) is not as easily discernible; hence, a comparison is presented in Fig. 8. All the data for the compared impellers were taken from the book published by Novák *et al.*[13] In the final analysis, the relative torque required by the Visco Jet® impellers was compared with the impellers from Fig. 7 and presented in Fig. 9.

Table 3 – *Comparison of dimensionless blending energy for various impellers in the region of developed turbulent flow. Comparison data published in*[13].

Impeller	$Pt_B^3 / \rho T^5$	Re
Visco Jet®– Classic	$2.9 \cdot 10^3$	above $2 \cdot 10^4$
Visco Jet®– Classic w. baffles	$3.7 \cdot 10^3$	above $2 \cdot 10^4$
Visco Jet®– Spiral	$2.4 \cdot 10^3$	above $3 \cdot 10^3$
Visco Jet®– Spiral w. baffles	$4.7 \cdot 10^3$	above $3 \cdot 10^3$
Rushton turbine	$1.8 \cdot 10^3$	above $2 \cdot 10^4$
6 Pitched blade	$0.7 \cdot 10^3$	above $2 \cdot 10^4$
4RLL	$0.3 \cdot 10^3$	above $2 \cdot 10^4$
Angel wings (TX 335)	$0.2 \cdot 10^3$	above $2 \cdot 10^4$

Drawing upon the findings of these comparisons with other impeller types, it can be concluded that both Visco Jet® impellers are of a general-purpose nature. The results indicate that neither impeller exhibits superior performance in any specific area over the other impeller types, with a negligible difference in performance observed between the two. In terms of their blending performance, the impellers appear to be optimally suited to more viscous fluids (approximately 0.75 Pa s), for which they demonstrate the most favourable outcomes, exhibiting performance comparable to that of the Anchor or Ribbon type impellers. Compared to these two impellers, Visco Jets® require a similar homogenisation energy while operating at several times lower torque values. This enables a more flexible application, as smaller, lighter support structures and drive systems are required. This reduces the overall cost and complexity of the design of the system. However, at lower viscosities, the Visco Jets® were outperformed by all the compared impellers, particularly those of the hydrofoil type. These results appear to align with the marketing materials available on the manufacturers' website, where both impellers are primarily promoted for use with viscous fluids (up to 30 and 100 Pa s). This focus might justify their somewhat diminished performance in regions of developed turbulent flow. Consequently, in terms of blending capabilities, they are particularly well-suited for processes where a wide range of viscosities must be addressed by a single impeller. An example of such processes would be paint homogenisation, syrup dilution, crystallisation processes, or any application where universal lightweight transportable solution is necessary.

A comparison of the two models indicates that the Visco Jet® Spiral is marginally more effective in blending applications at the upper and lower limits of the tested range of Reynolds numbers. Conversely, the Classic model exhibits a slight advantage in the transition region. This discrepancy can be attributed to the presence of turbulent mixing around the helically wound wire and the more pronounced radial flow facilitated by the gaps between the wires, particularly at high Re values. The discrepancy in the creeping flow region may be attributed to imprecise measurement, as evidenced by the confidence intervals. With a more extensive dataset, the regression for the Visco Jet® Classic presented in Fig. 4 could approach that of the Visco Jet® Spiral. The suitability of the impeller for highly viscous fluids (100 Pa s) remains to be determined, as the maximum viscosity tested was 30 Pa s. However, other impeller types from the comparison chart appear to be more suitable for such applications. An additional improvement in the blending process within the creep flow region could be achieved by optimising the placement of the impeller. Standard placement (height of the impeller above the vessel's bottom) of the impellers appeared to impede their ability to effectively expand the mixing loop towards the fluid surface. As a result, the last place to retain the colourant was usually found to be close to the fluid's surface or the shaft. When the impellers were placed toward the centre of the vessel, the discoloured state was reached more evenly throughout the volume of the vessel. The effect of baffles on the blending process was also surprising. Given the recommendation of impellers for use with IBC containers[2], it could be expected that they would perform better in configurations with standardly placed baffles. This is usually the case for most impellers for which integral properties (Power number, dimensionless homogenisation time) tend to be similar between the two geometries[14–16]. However, the addition of baffles has a detrimental effect on both Visco Jet® impellers and should be avoided. Nevertheless, the Visco Jet® impellers could still perform well in rectangular vessels, due to the fundamental difference in the underlying macroscopic flow pattern. That is because the flow pattern in rectangular vessels is more defined by greater tangential flow than in their cylindrical equivalents[17]. This may prove beneficial for Visco Jet® impellers, as they have been shown to perform better under such conditions. However, this hypothesis must first be confirmed experimentally. Due to these reasons, the presented results cannot be extrapolated to rectangular vessels, as is sometimes the case with other impellers.

In terms of suspension characteristics, Visco Jet® Classic appears to be more suited for particle suspension, primarily due to its reduced drag at higher rotation speeds (developed turbulent flow),

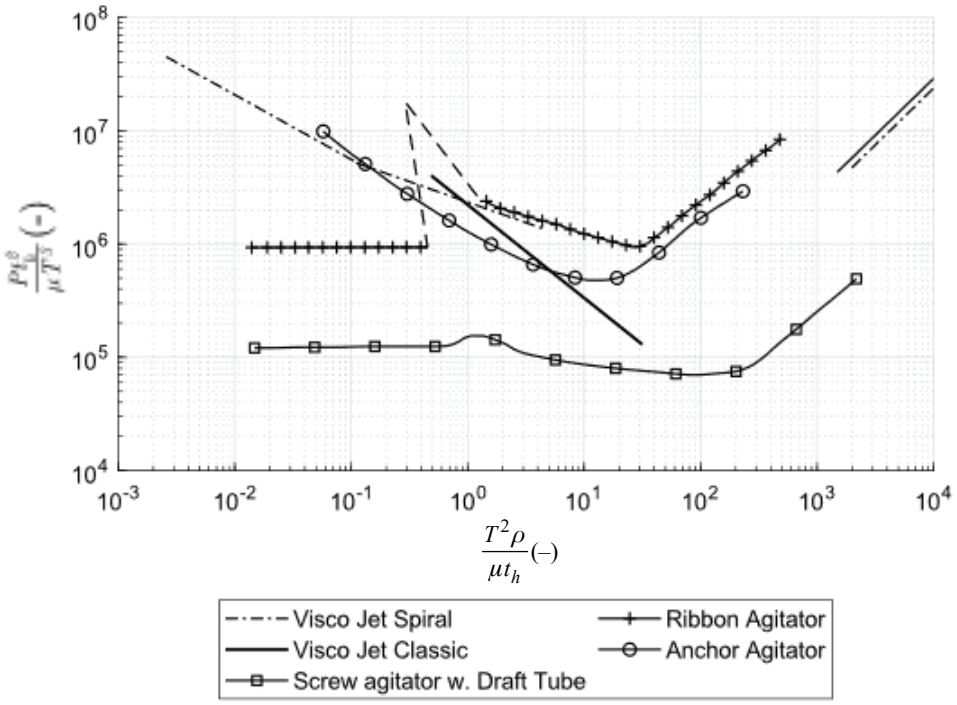

Fig. 8 – *Comparison of the dimensionless homogenisation energy for various impellers in the creeping flow region. Comparison data published in*[13].

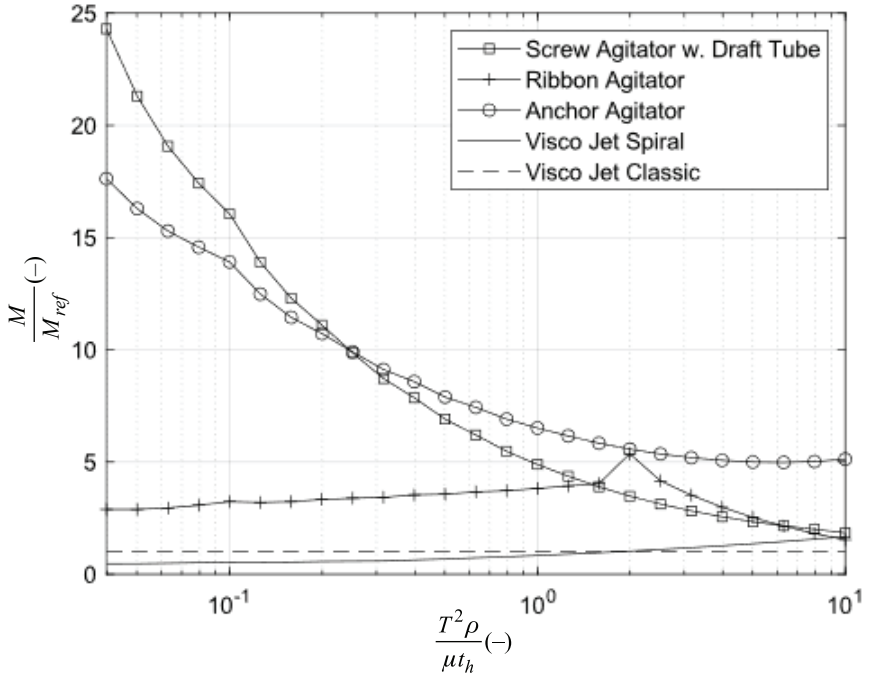

Fig. 9 – *Comparison of the relative torque requirements of various impellers in the creeping flow region with Visco Jet® Classic as reference. Comparison data published in*[13].

especially in baffled or partially baffled systems. The primary benefit of the Visco Jet® impeller is its independence from the power input necessary to reach the just-suspended state on particle concentration, thus making it more suitable for suspensions with high particle concentration.

When the objective is to achieve a just-suspended state, the unbaffled configuration is the most energy efficient. However, this configuration is unable to fully homogenise the batch before air suction into the impeller occurs. This can be mitigated by incorporating baffles into the system. Al-

though this modification increases the rotation speed at which the just-suspended state is achieved, and thus a greater power input is necessary, the semi-submerged baffle system offers an acceptable compromise between these two options. It enables the system to reach a fully homogenised state, while it only marginally increases the minimum rotation speed required for the just-suspended state. In this configuration, the baffles must be positioned above the upper edge of the impeller cones. This configuration enables the large swirling motion to be present in the bottom part of the vessel, which appears to be the primary mechanism behind the enhanced performance of the unbaffled system. In the upper half, this motion is disrupted by the presence of baffles, thus enabling higher rotation speeds necessary to achieve the fully homogenised state.

As demonstrated by the findings presented in this study, both Visco Jet® impellers exhibit a behaviour that defies expectations. If these phenomena are not properly addressed, they have the potential to result in suboptimal designs. However, both Visco Jet® impellers appear to exhibit sufficient flexibility to yield at least some results, even when applied improperly.

Conclusions

In this study, the blending and suspension characteristics of two Visco Jet® impellers were examined. Contrary to the manufacturer's claims, a typical flow pattern for radial impellers was observed. For fluid-blending applications, both impellers were found to be more effective with more viscous fluids (0.75 Pa s and higher), yielding comparable results to other tested impellers. However, for less viscous fluids (around 1 mPa s and lower), all standard lower viscosity impellers (hydrofoils, pitch blades) demonstrated superior performance compared to both Visco Jet® impellers. Of the two tested variants, the Visco Jet® Spiral outperformed the Classic version in terms of blend applications across the majority of the examined impeller Re numbers. This might be primarily due to the increased local turbulence around the helically wound wire of the impeller cone, creating more drag resistance and accelerating the blending process. However, a more in-depth study, incorporating a CFD simulation, would be necessary to provide a comprehensive description of this phenomenon. This effect diminishes when operating in the creeping flow region, where, given the existing uncertainties, both impeller types exhibited similar, if not identical, capabilities.

In the context of particle suspension, the Visco Jet® Classic emerges as a superior alternative due to the reduced drag on its impeller cone, while it generates a comparable momentum in the fluid as its spiral counterpart. Notably, the concentration of particles in the suspension exhibited minimal impact on power input, at which the just-suspended state was attained. This attribute makes the impeller particularly well suited for suspensions with high particle concentrations. The unbaffled configuration required the least power input to reach the just-suspended state. However, in this configuration, the impeller was unable to achieve full homogeneity without the presence of baffles, because of the presence of a large axial vortex. If a fully homogenised suspension is desired, it is suggested that a partially submerged baffle system is used, where the bottom of the baffles is above the upper edge of the impeller. This configuration, when compared to the fully baffled system, lowers the power input necessary to achieve the desired just-suspended state. However, the baffles still disrupt the large axial vortex, enabling the system to attain the higher rotation speeds necessary for a fully homogenised suspension.

Drawing upon the findings of this study, it can be concluded that the primary benefits of the two Visco Jet® impellers are their versatility in operating under diverse conditions and their simple maintenance. These impellers possess a simple, easy to clean geometry, and are well-suited for unbaffled vessels, operating optimally under conditions of high rotation speed and low torque.

As a result of the aforementioned reasons, the agitation system incorporating these impellers is more slender and straightforward to design and manufacture, while it preserves comparable mixing characteristics. This renders the impellers ideal for complex mixing applications where a wide range of flow characteristics must be covered, such as the dissolution of viscosity-changing compounds or the blending of fluids with significantly different viscosities (syrup dilution, paint homogenisation, etc.), or as a general portable mixer for viscous fluids. However, for common uniform applications, better hydrodynamically optimised impellers are available for all mixing regions reviewed in this article. For viscous fluids (above 6 Pa s) both screw and ribbon impellers are more energy efficient, but require higher torque values to operate. For blending of low-viscosity (1 mPa s) fluids all optimised hydrofoils have better performance.

Symbols

C – impeller clearance, m
D – impeller diameter, m
H – vessel height, m
L – baffle of bottom clearance, m
M – shaft torque, N m
M_{ref} – reference shaft torque of Visco Jet® Classic, N m
n – impeller rotation speed, s^{-1}
t_B – blending time, s
T – vessel diameter, m
W_b – baffle width, m
$\Delta\rho$ – solid – liquid density difference, kg m^{-3}
ρ – liquid density, kg m^{-3}
ρ_{su} – suspension density, kg m^{-3}

Dimensionless numbers

A_i – regression parameter
B_i – regression parameter
Fr' – modified Froude number
Po – Power number
Re – impeller Reynolds number

Impeller/abbreviations

6SL – 6-bladed impeller pitched at 45° [8]
3SL – 3-bladed impeller pitched at 45° [8]
3RLL – 3-bladed impeller with changing pitch angle[18]
4RLL – 4-bladed impeller with changing pitch angle[19]
A310 – SPX FLOW ® Lightnin A310 Hydrofoil Impeller
Marine propeller – EKATO ® Marine propeller (discontinued)[8]
TX 335 – Angel wings impeller[20]

FUNDING

"This research was funded by Student Grant Competition of CTU in Prague, grant number: SGS23/160/OHK2/3T/12"

References

1. *Rahimi, M., Amraei, S., Alsairafi, A. A.*, Experimental and computational fluid dynamics modeling of mixing by Visco-jet impellers, Korean J. Chem. Eng. **28** (2011) 1372.
2. *GmbH, V. J. R.*, VISCO JET® AGITATOR TECHNOLOGY, URL: https://viscojet.de/en/innovations/ (8.10.2024)
3. *Paul, E. L., Atiemo-Obeng, V. A., Kresta, S. M.,* (Eds.) Handbook of Industrial Mixing, Wiley, Hoboken, N.J.; Great Britain, 2003. doi: https://doi.org/10.1002/0471451452
4. *Medek, J., Fořt, I.*, Pumping effect of impellers with flat inclined blades, Collect. Czechoslov. Chem. Commun. **44** (1979) 3077. doi: https://doi.org/10.3390/en15020585
5. *Rieger, F., Jirout, T., Ceres, D., Pešl, L.*, Homogenization and suspension efficiency of hydrofoil impeller TX 535, in Kluson, P. (Ed.), CHISA 2012. Prague, Czech Republic, 25 – 29 August 2012, Curran, Red Hook, NY, 2013.
6. *Zwietering, Th. N.*, Suspending of solid particles in liquid by agitators, Chem. Eng. Sci. **8** (1958) 244. doi: https://doi.org/10.1016/0009-2509(58)85031-9
7. *Myers, K. J., Fasno, J. B.*, The influence of baffle off-bottom clearance on the solids suspension performance of pitched-blade and high-efficiency impellers, Can. J. Chem. Eng. **70** (1992) 596. doi: https://doi.org/10.1002/cjce.5450700326
8. *Jirout, T., Rieger, F.*, Impeller design for mixing of suspensions, Chem. Eng. Res. Des. **89** (2011) 1144. doi: https://doi.org/10.1016/j.cherd.2010.12.005
9. *Rieger, F., Ditl, P.*, Suspension of solid particles, Chem. Eng. Sci. **49** (1994) 2219. doi: https://doi.org/10.1016/0009-2509(94)E0029-P
10. *Taghavi, M., Moghaddas, J.*, Using PLIF/PIV techniques to investigate the reactive mixing in stirred tank reactors with Rushton and pitched blade turbines, Chem. Eng. Res. Des. **151** (2019) 190. doi: https://doi.org/10.1016/j.cherd.2019.08.016
11. *Stelmach, J.*, Mixing power and hydrodynamics for different clearances of the flat blade turbine impeller, Chem. Process Eng.-N. F. (2023) **7** doi: https://doi.org/10.24425/cpe.2023.144693
12. *Montante, G., Lee, K. C., Brucato, A., Yianneskis, M.*, Experiments and predictions of the transition of the flow pattern with impeller clearance in stirred tanks, Computers and Chemical Engineering, Vol. 25. URL: www.elsevier.com/locate/compchemeng
13. *Novák, V., Rieger, F., Vavro, K.*, Hydraulické pochody v chemickém a potravinářském průmyslu, SNTL, Praha, 1989.
14. *Xanthopoulos, C., Stamatoudis, M.*, Turbulent range impeller power numbers in closed cylindrical and square vessels, Chem. Eng. Commun. **46** (1986) 123. doi: https://doi.org/10.1080/00986448608911401
15. *Novák, V., Rieger, F.*, Mixing in vessels of square cross-section, Collect. Czechoslov. Chem. Commun. **38** (1973) 350. doi: https://doi.org/10.1135/cccc19730350
16. *Kresta, S. M., Mao, D., Roussinova, V.*, Batch blend time in square stirred tanks, Chem. Eng. Sci. **61** (2006) 2823. doi: https://doi.org/10.1016/j.ces.2005.10.069
17. *Jirout, T., Jiroutova, D.*, Designing of Mixing Equipment, Reactors and Bioreactors, in Dynybyl, V. (Eds.), The latest methods of construction design, Springer Berlin Heidelberg, New York NY, 2015. pp 19–26. doi: https://doi.org/10.1007/978-3-319-22762-7_4
18. *Jirout, T., Rieger, F., Rzyski, E.*, Mieszadła z łamanymi łopatkami. Wpływ liczby łopatek na wytwarzanie zawiesin, Inżynieria i aparatura chemiczna **41** (2002) 53.
19. *Jirout, T., Rieger, F.*, Axial agitator with large-areas broken blades, Utility Model, (2012).
20. *Rieger, F., Jirout, T., Ceres, D., Seichter, P.*, Effect of impeller shape on solid particle suspension, Chem. Process Eng. **34** (2013) 139. doi: https://doi.org/10.2478/cpe-2013-0012